PCCP

Accepted Manuscript

ROYAL SOCIETY OF CHEMISTRY

www.rsc.org/pccp

Journal Name

RSCPublishing

ARTICLE

Electronic structure of graphene nanoribbons doped with nitrogen atoms: a theoretical insight.

Cite this: DOI: 10.1039/x0xx00000x

A.E. Torres and S. Fomine*

Received ooth January 2012,
Accepted ooth January 2012

DOI: 10.1039/x0xx00000x

www.rsc.org/

The electronic structure of graphene nanoribbons doped with graphitic type of nitrogen atoms has been studied using B3LYP, B2PLYP and CAS methods. In all but one case the restricted B3LYP solutions were unstable and CAS calculations evidence multiconfigurational nature of the ground state contributing with two dominant configurations. The relative stability of doped nanoribbons depends mostly on the mutual position of dopant atoms and notably less on the position of nitrogen atoms within the nanoribbon. N-graphitic doping affects cationic states much more than anionic ones due the participation of the nitrogen atoms in the stabilization of the positive charge resulting in drop of ionization energies (IPs) for N-graphitic doped systems. Nitrogen atoms do not participate in the negative charge stabilization of anionic species and, therefore, the doping does not affect the electron affinities (EAs). Unrestricted B3LYP method is the method of choice for the calculation of IPs and EAs. Restricted B3LYP and B2PLYP produces unreliable results for both IPs and EAs while CAS strongly underestimates the electron affinities. This is also true for the reorganization energies where restricted B3LYP produces qualitatively incorrect results. Doping changes the reorganization energy of the nanoribbons; the hole reorganization energy is generally higher than the corresponding electron reorganization energy due to the participation of nitrogen atoms in the stabilization of the positive charge.

Introduction

Recently, graphene has been widely investigated due to its unique physical and electronic properties, since it could represent one of the most promising materials for its implementation in electronic devices.[1,2] It is the research on graphene that unleashed the investigations in the area of graphene nanoribbons. The graphene nanoribbons (GNRs) are graphene stripes of nanometric size that in contrast to their parent structure were predicted to have a band gap, opening a new field of application in digital electronics.[3] It is inferred that the structures fabricated from GNRs (that are just a few nanometres wide) will become key elements for nanoelectronics. Nowadays these structures have been synthetized and they were found to have higher electron mobilities compared to graphene.[4-6]

The properties of GNRs are governed by their geometric parameters and chemical composition. In this regard, the chemical doping is an important strategy for tuning the electronic properties of graphene and the modification the energy gap, similar to that developed for the silicon based technology.[7] One of the most employed methods is the substitutional doping, where heteroatoms such as nitrogen or boron replace some of the carbon atoms of the sp^2 lattice of graphene. In particular, nitrogen has approximately the same atomic radii as carbon and one extra electron, thus modifying its electronic and transport properties.[3,8]

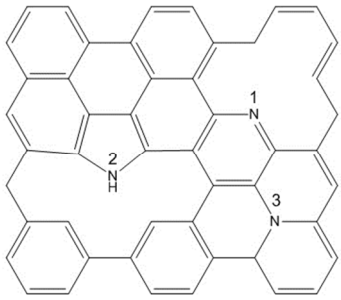

Fig. 1 Nitrogen doping sites in a GNR model structure: pyridinic (1), pyrrolic (2) and graphitic (3).

N-doped graphene nanoribbons have recently been studied both experimentally and theoretically. It was found that the nitrogen doping effect depends on the doping site. The most common types of nitrogen in the hexagonal carbon lattice are the graphitic, pyridinic and pyrrolic.[9-12] (Fig. 1)

It was predicted that N-pyridinic and N-pyrrolic doping of graphene is a *p*-type doping, while graphitic nitrogen induces *n* type of conductivity.[8] The assignment of N-pyrrolic doping to the *p* type is, however, rather questionable. It is well known that pyrrolic nitrogen is a strong electron-donating group due to the lone pair of the nitrogen atom interacting with π-electrons of

the GNR. Pyrrole itself and the related polycyclic heterocycles like carbazole are very reactive towards the electrophiles, characteristic of *n*-doped systems. Moreover, both graphitic and pyrrolic nitrogens have lone pairs and, therefore, should possess similar electron-donating properties.

It has been suggested earlier that large aromatic polycyclic hydrocarbons and GNRs type structures have multiconfigurational polyradical character of their ground state.[13-15] On the other hand, it seems that single reference wavefunction describes well the ground state of polycyclic hydrocarbons when dynamic correlation is properly taken into account.[16-20]

Previously, we have performed a systematic study of the electronic structure of the above mentioned systems. It has been found that multiconfigurational character of the ground state increases with the size of the system and do not necessarily implies a multiradicalic character of the ground state found only for very large systems.[21] Therefore, motivated by the previous results we decided to analyze the effect of nitrogen doping on the electronic properties of the nanoribbon type structures taking into account their notable multiconfigurational character, which is important to consider for the correct description of the electronic structure and accurate prediction of its properties.

Computational Details

The geometry optimizations were carried out using D3 dispersion corrected [22] B3LYP functional as implemented in Turbomole 6.6 [23] in conjunction with Dunning's correlation consistent cc-pVDZ basis set.[24] The geometries of all the structures have been optimized for singlets and triplets using restricted and unrestricted methods, respectively. When triplet instability has been detected for the closed shell singlet state, the geometry was reoptimized using broken symmetry unrestricted method (UB3LYP). Single point energy calculations using B2PLYP functional[25] were carried out for singlet state too using restricted and unrestricted reference wavefunction to study the importance of nonlocal dynamic correlation.

To evaluate the multiconfigurational character of the studied systems, CAS single point energy calculations were carried out using B3LYP optimized structures of the corresponding multiplicity using active spaces consisting of 10 electrons and 10 orbitals, for neutral species, 9 electrons and 10 orbitals for cation radicals and 11 electrons and 10 orbitals for anion radicals, respectively. This active space was the largest practical active space possible. For all the atoms the 6-31G (d) 5d basis set [26] was used. All active orbitals were carefully analyzed to ensure that *p* electron of nitrogen atoms were included into the active space. These calculations were carried out with Gaussian 09 rev. D.01 code. [27] The geometry of the studied GNR is shown in Fig.2. This GNR has been synthesized experimentally. [28]

The doping effect of graphitic and pyridinic nitrogens has been studied. According to a previous paper [21] the ground state of similar systems possesses a notable multiconfigurational character, with only moderate polyradical character since the most important contributions to the multireference wavefunction come from closed shell singlet configurations.

The graphene nanoribbon model selected to evaluate the nitrogen doping effect has an armchair structure with N (width) =9, commonly named 9-AGNR. According to the previously reported nomenclature for rectangular polycyclic hydrocarbons [21] of dimensions **m**x**n** where **m** and **n** are the number of fused benzene rings in columns and rows, this structure corresponds to a rectangular graphene nanoribbon of 4x6 (R4,6). The amount of nitrogen incorporated in the pristine structure is of about 1.4% (atomic; 2 nitrogen atoms) corresponding to the experimental reported values for graphitic doping.[29,30]

The structures of doped graphene nanoribbons are shown in Fig.2.

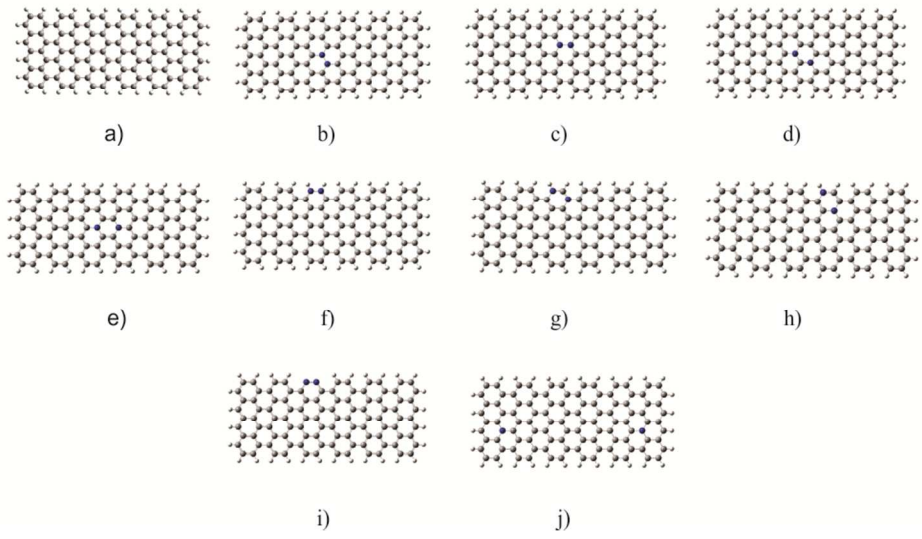

Journal Name

RSCPublishing

ARTICLE

Fig. 2 Pristine (**a**) and doped in core or edges graphene nanoribbon structures

The doping sites for graphitic nitrogen were chosen to cover the maximum number of nonequivalent positions where nitrogen atoms are still interacting with each other. Therefore, the maximum separation between nitrogen has been set to 2 carbon atoms. These structures were found to be the most common in nitrogen doped graphene.[31] Moreover, to explore the effect of the doping site type and the separation between doping sites, systems **i** and **j** have been also studied. System **i** has pyridinic type of doping sites, while in model **j** nitrogen atoms are separated from each other.

The hole reorganization energies (λ_+) of GNRs were estimated as following:

$$\lambda_+ = (E_n^+ - E_n) + (E_+^n - E_+)$$

Where E_n and E_+ are the energies of the neutral and cationic species in their lowest energy geometries, while E_n^+ and E_+^n are the energies of the neutral and cationic species with the geometries of the cationic and neutral species, respectively. The electron reorganization energy (λ_-) is defined similarly:

$$\lambda_- = (E_n^- - E_n) + (E_-^n - E_-)$$

In this case, E_n and E_- are the energies of the neutral and the anionic species in their lowest energy geometries, while E_n^- and E_-^n are the energies of the neutral and anionic species with the geometries of the anionic and neutral species, respectively.

Results and discussion

The relative energies of singlet states calculated for nitrogen doped graphene nanoribbons (N-GNRs) are shown in the Table 1. The stability test performed for restricted B3LYP solutions detected for all but **j** neutral species triplet instability, therefore, polyradicalic states (PRS) with the multiplicity 1 were also optimized using UB3LYP. UDFT produces unphysical spin densities since unrestricted Hamiltonian does not commute with S^2 operator. However, due to the nature of broken symmetry unrestricted wavefunction it describes better multireference systems than restricted wavefunction does. Following the variational principle unrestricted solution is better approximation to the exact wavefunction since it produces lower energy state.

The lowest energy structure at B3LYP level (**j**) was taken as a reference. As seen from the Table 1 the stability order of the structures depends on the method. The best correlation is observed between UB3LYP and CAS methods; predicting **c** being the highest energy isomers. Similar order of stability was also reported for N-doped graphene sheets.[31] As seen from the Table 1 B2PLYP results are very different from both CAS and B3LYP. Given the obtained results it must be noted that *para* N-GNR are the most energetically stable structures compared with the other N-GNRs. On the other hand, the least stable structures are the *ortho* ones. This is definitely related with much weaker N-N bond existing in *ortho* isomers compared to C-C and C-N bonds of *para* and *meta* doped structures.[32] As seen from Table 1 the energy difference between the most stable and the less stable isomer is very important achieving various tenths of kcal mol^{-1} for all theory levels. Therefore, the doping topology affects enormously the relative energy of the doped systems. Doping changes the nature of the lowest energy state in two cases at CAS level. Thus, for the structures **b** and **h** the lowest energy state is not singlet as for other systems, but triplet state. In the case of DFT level of theory PRS and triplet states are degenerated within 0.1-0.2 kcal mol^{-1} for all systems.

Table 1. Relative electronic energies calculated for N-GNRs (kcal mol^{-1}). RB3LYP/cc-pVDZ optimized closed shell singlet (S0) and UB3LYP/cc-pVDZ polyradicalic state (PRS). S0 geometries were used for single point CAS(10,10)/6-31G(d) (CAS) and B2PLYP/cc-pVDZ calculations.

GNR	Relative energy			
	S0	CAS	PRS[a)]	B2PLYP
b	44.6	40.7[b)]	27.0	0.0
c	48.2	56.2	31.2	60.8
d	34.0	50.5	17.1	43.6
e	16.1	18.2	-2.0	22.5
f	18.8	69.4	1.2	26.7
g	22.3	27.4	4.3	40.1
h	7.3	0.0[b)]	-9.9	17.1
i	-	-	-	-
j	0.0	28.7	0.0	42.3

a) S0 B3LYP energies of **j** structure is taken as reference for the relative energy calculations at B3LYP level.

b) Triplet states for these structures are the most stable ones at CAS level

Table 2 shows the most important configurations contributing to S0 multireference wavefunction of pristine and doped GNRs. S0 and PRS geometries were used for single point energy evaluation at CAS/6-31G(d) level. It should be noted, that for **b** and **h** structures S0 is not the ground state according to CAS, and these data are presented here just for comparison purpose. All systems except **j** show clear multireference character. Only for two of them the systems

squared CI expansion coefficient for S0 exceeds 0.46. System **j**, however, has single reference ground state as follows from the stability of the restricted solution and only one dominant configuration to the CAS wavefunction.

In all other cases doping with nitrogen atoms does not change multiconfigurational character of the GNRs, since the most important configurations that appear for the pristine structure are found in the doped systems too contributing with the same weigh (two dominant closed shell configurations contribute to the singlet state with more than 80%). For systems **c**, **d** and **g**, however, doping promotes polyradicalic character of the ground state where the contribution of two above mentioned configurations drops to only 64%, the rest of configurations are polyradicalic (mainly di- and tetra-radicalic). It has been shown,[21] that the multiconfigurational character of the electronic state for fused aromatic hydrocarbons decreases with multiplicity. Thus, for systems **b** and **h** where the ground state is triplet, squared CI expansion coefficients for the dominant triplet configuration are of 0.84 and 0.83, respectively, indicating mostly single reference character of these states.

Table 2 demonstrates that there is no significant difference in dominant configurations of the active space between the closed shell S0 and open shell PRS geometries. The only important variations are for structures **f** and **g** where the geometry choice notably affects the multireference wavefunction.

Table 3 shows ionization potentials (IPs) and electron affinities (EAs) of GNRs calculated using different methods.

As it could be seen, at DFT level PRS reference state produces notably higher IPs and lower EAs, compared to S0, reflecting significantly lower total energies of PRS state compared to S0 one. According to DFT results, N-graphitic doping leads to a drop in IPs, while pyridinic nitrogens increase IP (model **i**). The most pronounced decrease in the IP was detected for *meta* (**d**) structure. Since no experimental data are available for IPs of GNRs we were only able to compare the calculated IPs with graphene work function (4.3 eV[33]). As seen, graphene work function is very close to calculated IP for pristine GNR (**a**) estimated with restricted S0 state as a reference state (4.43 eV). It is well known, however, that IPs of conjugated systems drop with number of atoms involved in the conjugation.

Therefore, the use of restricted S0 state as the reference state for IPs definitely underestimates IP for GNR **a**. IPs estimations using CAS must be much close to the real values, since it has been shown that CAS produces IPs for conjugated hydrocarbons only several tenths of eV higher than experimental values.[34] According to CAS, IP of pristine GNR (**a**) is 5.75 eV, while UB3LYP predicts 5.19 eV. Considering the above it seems that UB3LYP method gives reasonable estimation of IP in spite of strong spin contamination existing in the neutral state ($<S^2>$ = 2.11, Table 5) compared to restricted B3LYP.

Table 2. Squared CI expansion coefficients for dominant configurations in GNRs at CAS(10,10)/6-31G(d) level of theory for closed shell singlet (S0) and polyradicalic state (PRS) optimized structures, respectively.

GNR (S0)	2222200000 [a)]	2222020000 [a)]	GNR(PRS)	2222200000 [a)]	2222020000 [a)]
a	0.42	0.42	a	0.42	0.42
b	0.43	0.43	b	0.43	0.43
c	0.32	0.32	c	0.32	0.32
d	0.32	0.32	d	0.32	0.32
e	0.42	0.42	e	0.42	0.42
f	0.84	0.00	f	0.41	0.41
g	0.32	0.32	g	0.14	0.53
h	0.41	0.41	h	0.40	0.40
i	0.46	0.46	i	0.45	0.45
j	0.85	0.00	j	-	-

a) Electron distribution in active orbitals of dominant configurations

Table 3. Adiabatic ionization potentials (IP) and electron affinities (EA) estimated at CAS(10,10)/6-31G(d) (CAS), B2PLYP/cc-pVDZ (B2PLYP), RB3LYP/cc-pVDZ (S0) and UB3LYP/cc-pVDZ (PRS) levels (eV).

GNR	IP S0	IP PRS	IP CAS[a)]	IP B2PLYP[a)]	EA S0	EA PRS	EA CAS[a)]	EA B2PLYP[a)]
a	4.43	5.19	5.75	6.68	-2.90	-2.13	0.37	0.08
b	3.89	4.65	6.38[b)]	9.19	-2.83	-2.07	0.63[b)]	2.12
c	3.76	4.49	3.63	6.07	-2.85	-2.11	1.11	-1.03
d	3.54	4.27	6.04	6.65	-2.82	-2.08	0.92	-0.31
e	3.96	4.74	6.22	6.39	-2.84	-2.06	0.76	-0.78
f	3.92	4.68	4.19	6.83	-2.85	-2.08	-1.20	0.17
g	3.61	4.39	3.96	5.42	-2.82	-2.04	0.42	-0.56
h	3.84	4.58	6.25[b)]	6.13	-2.84	-2.09	0.39[b)]	-0.27
i	4.51	5.27	5.92	4.79	-2.96	-2.19	0.41	-2.75
j	4.55	-	5.94	5.61	-2.10	-	0.06	-1.55

a)RB3LYP/cc-pVDZ and UB3LYP/cc-pVDZ geometries were used for the calculations of neutral molecule and cation, respectively

b) The triplet state was taken as a reference for the neutral structure.

The overestimation of the neutral state energy, taking place for the restricted B3LYP method will lead also to the overestimation of EA. As seen, EAs calculated using restricted S0 energy as a reference is almost 1 eV higher compared to these calculated with PRS state.

Moreover, anion radicals have low spin contamination (Table 5) which produces more reliable EA's for the studied systems. CAS however, strongly underestimates EAs due to significant difference in dynamic correlation between neutral and anionic state [35] predicting positive electron affinity for most of the studied systems. B2PLYP produces very high and unreliable IPs in the most of the cases and positive or weakly negative EAs. This is probably related to the lack of static correlation in this method and the low "quality" of the closed shell reference wavefunction.

IPs are the most affected by doping, while EAs barely change when carbons are replaced by nitrogens. EAs slightly decrease in case of graphitic doping and increase for pyridinic doped system **i**. This is due to the fact that the lone electron of graphitic nitrogen is relatively weakly bounded, decreasing IP of the doped system. As an example Fig. 2 shows that the unpaired spin density distribution in cation radical of **d** structure involves 2 nitrogen atoms, whereas no nitrogen atoms are involved in anion radical stabilization.

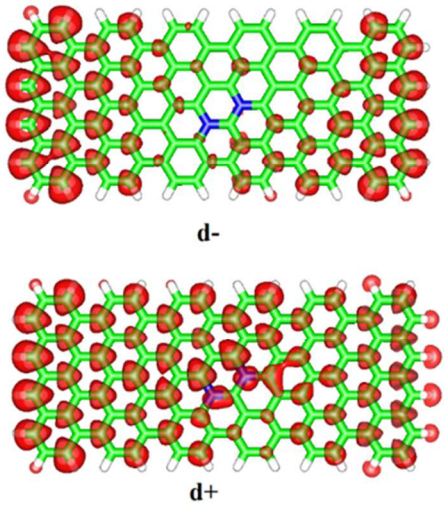

Fig. 3 Spin density distribution in anion and cation radicals for **d** structure

Table 4. Squared CI expansion coefficients for dominant configurations in cation (C_+^2) and anion radicals (C_-^2) at CAS(9,10)/6-31G(d) and CAS(11,10) levels of theory. The difference of natural charges for nitrogen atoms between cationic and neutral (Δ^+) and anionic and neutral (Δ^-) states at UB3LYP/cc-pVDZ level of theory

molecule	C_+^2	Configuration	Δ^+	C_-^2	Configuration	Δ^-
a	0.94	2222a00000 [a)]	-	0.94	222220a000 [a)]	-
b	0.98	2222a00000 [a)]	0.100	0.94	22222a0000 [a)]	-0.006
c	0.94	a2220ab000 [a)]	0.119	0.98	222a220000 [a)]	-0.005
d	0.98	2222a00000 [a)]	0.015	0.98	22222a0000 [a)]	-0.003
e	0.98	2222a00000 [a)]	0.102	0.98	222220a000 [a)]	-0.008
f	0.96	a22200b00a [a)]	0.145	0.98	22222a0000 [a)]	-0.010
g	0.34	2a2abab000 [a)]	0.050	0.90	22222a0000 [a)]	0.000
h	0.94	a2220ab000 [a)]	0.139	0.92	222220a000 [a)]	-0.009
i	1.00	2222a00000 [a)]	0.014	1.00	22222a0000 [a)]	-0.015
j	1.00	2222a00000 [a)]	0.004	0.90	22222a0000 [a)]	-0.03

a) Electron distribution in active orbitals of dominant configurations

Table 4 shows the contributions of the dominant configurations to the multiconfigurational wavefunction of the cation and anion radicals obtained from CAS calculations and the difference of natural charges for nitrogen atoms between neutral and charged N-GNRs. Unlike neutral GNRs most of the charged systems can be described with only one dominant configuration except for **g+** where the dominant configuration contributes only 32%. For some of the positively charged N-GNRs the dominant configuration is polyradicalic as seen for cation radicals **c**, **f**, **g** and **h**. All anion radicals are, however, well described by only one configuration with an unpaired electron. This difference can also be seen from the Table 5 where $<S^2>$ expectation values are listed for the neutral, cationic and anionic species of GNRs calculated at UB3LYP level. The spin contamination for cation radicals of graphitic doped GNRs is always higher than that for the corresponding anion radicals indicating higher polyradicalic character of cationic species. This difference resides in the character of the delocalization of the polarons in cation and anion radicals. Fig. 3 shows a typical case where the electrons of nitrogen atoms participate in the stabilization of the cation radicals but not the anion radicals. This increases the polyradicalic character of the

cation radicals compared to anion radicals, which reflects also increased spin contamination of doped cation radicals compared to the anion radicals in the case of graphitic doping (Table 5). It is noteworthy that for pristine structure **a** the spin contamination is small and similar for both cation and anion radicals, thus demonstrating the effect of graphitic nitrogen doping on the polyradicalic character of cation radicals of N-GNRs. Similar conclusion can be made analyzing the charge differences on nitrogen atoms between cationic, neutral and anionic states. As seen from the Table 4, the charges on nitrogen atoms are practically the same in neutral and anionic state, while in the case of cations, nitrogen atoms participate actively in the stabilization of the positive charge. Thus, in the case of **h+** some 14% of positive charge is located on only two nitrogen atoms while the rest of positive charge is delocalized over the rest 106 carbons of N-GNR. In case of pyridinic type of doping nitrogen atoms do not participate in the stabilization of the positive charge in cation radicals as follows from the Table 4.

Table 5. $<S^2>$ expectation values for GNRs for neutral (NEU), cationic (CAT) and anionic (ANI) species at B3LYP/cc-pVDZ level.

GNR	NEU	CAT	ANI
a	2.11	0.80	0.78
b	1.11	1.86	0.79
c	1.22	1.86	0.79
d	1.52	1.91	0.94
e	1.11	1.84	0.79
f	1.16	1.87	0.79
g	2.08	1.85	1.59
h	1.12	1.86	0.79
i	1.12	0.79	0.79
j	0.00	0.83	0.77

An important point in understanding of the conductivity of doped GNRs is to characterize structural factors essential in the charge transfer rates. Thus, it has been demonstrated that the solid-state hole mobility in arylamines is related to the internal reorganization energy. Low internal reorganization energies of isolated molecules have been associated with higher solid-state charge carrier mobility (when combined with large electronic coupling) critical for the development of high efficiency electronic devices. It is known that most organic semiconductors have internal reorganization energies greater than 0.1 eV. Interestingly, several *p*-type organic semiconductors have been reported with internal reorganization energies (λ_+) of less than 0.1 eV. However, only a few π-type acceptors with electron reorganization energies (λ_-) of less than 0.1 eV, including fullerene C_{60} (0.060 eV), are known.[36] The reorganization energy decreases with increasingly large conjugated cores; for example, for triphenylene it is 0.18 eV, for coronene 0.13 eV and for hexa-peri-hexabenzocoronene 0.1 eV.[37-39]

The charge transport mechanism in GNRs depends on its size. Thus, in the case of large GNR (40 nm wide) the ballistic mechanism is operational.[5] However, for smaller systems all experimental data point to hopping mechanism.[40]

Table 6 summarizes calculated λ_+ and λ_- for pristine and doped GNRs. Since the closed shell singlet solution is not stable for neutral GNRs at B3LYP level due to multiconfigurational character of the ground state, UB3LYP along with RB3LYP method were used for the calculations of E_n, E_n^- and E_n^+ energies. RB3LYP method produced converged solutions only for **b**, **g** and **h** systems. To the best of our knowledge there is no available experimental data on reorganization energy of pristine or doped GNRs. However, it is reasonably to suggest that the reorganization energies of pristine GNR must be of the order of 0.1 eV or less, moreover, it has been demonstrated that B3LYP functional used for the reorganization energy calculations best reproduces the experimental data of organic conjugated systems.[41,42] As seen from the Table 6, RB3LYP method delivers unreliable reorganization energies (negative λ_- for doped system **g**). Random errors are introduced to the reorganization energy data due to unstable restricted solutions for E_n, E_n^- and E_n^+ energy calculation. Moreover, for most of the cases RB3LYP did not deliver converged solutions. UB3LYP method, on the other hand, gives physically meaningful results as seen from the Table 6. A very small and similar λ_- and λ_+ were calculated for pristine system **a**. Nitrogen doping notably affects the reorganization energies. Thus, doping in *meta* position (structures **d** and **g**) significantly increases both λ_- and λ_+. Systems **b**, **c** and **f**, where nitrogen atoms are in *ortho* position, forming explicit covalent bond between them, show an increase of λ_+, while λ_- remains very small. The reorganization energies of **e** and **h**, where nitrogen atoms are in *para* position to each other are affected less by doping compared to all other structures. As seen from the Table 6 the relative position of nitrogen atoms affects much more the reorganization energy than their position within GNR (core or edge). For the most stable structure **j** the reorganization energy is only slightly higher than that for pristine GNR, remaining notably low.

Table 6. Reorganization energies for electrons (λ_-) and holes (λ_+) (eV) estimated using UB3LYP and RB3LYP methods for neutral species, respectively.

GNR	UB3LYP/cc-pVDZ		RB3LYP/cc-pVDZ	
	λ_+	λ_-	λ_+	λ_-
a	0.021	0.020	-[a]	-[a]
b	0.274	0.004	0.010	0.317
c	0.104	0.009	-[a]	-[a]
d	0.335	0.330	-[a]	-[a]
e	0.077	0.002	-[a]	-[a]
f	0.101	0.037	-[a]	-[a]
g	0.248	0.201	0.063	-0.567
h	0.060	0.037	0.022	0.026
i	0.029	0.029	-[a]	-[a]
j	-	-	0.011	0.010

a) SCF not converged

Conclusions

The relative stability of N-GNRs is strongly related with mutual position of dopant atoms and much less with the position of nitrogen atoms within the nanoribbon. Doping does affect the multireference character of N-GNR in their neutral state. Thus,

for model **j**. where nitrogen atoms are well separated from each other the ground state is single reference. In spite of the significant multiconfigurational character detected for most of the singlet ground states, GNRs only exhibited two dominant closed shell singlet configurations. For the ionic species this is not the case and single reference methods give reasonable description. As a result single reference method does not provide well balanced description for both structures, thus giving too low IPs and too high EAs.

Graphitic nitrogen doping affects much more the cationic states compared to anionic ones due the participation of the nitrogen atoms in stabilization of the positive charge. This results in a drop of IPs of N-GNR. On the other hand nitrogen atoms do not participate in the negative charge stabilization of anionic species, thus not affecting EAs of N-GNRs. This is not the case for pyridinic doping (model **i**) where doping results in increase of IP and EA and, therefore, can be considered as *p* doping unlike *n* doping caused by graphitic nitrogen.

UB3LYP method is the method of choice for the calculation of IPs and EAs. Restricted B3LYP produces unreliable results for both IPs and EAs while CAS strongly underestimates the electron affinities. This shortcoming of CAS would definitely be repaired using perturbative correction to CAS energy. However, the computational cost of this correction is prohibitively high to implement for such large systems. B2PLYP overestimates IP and underestimate EAs of GNRs probably due to the low "quality" of the closed shell reference wavefunction and lack of static correlation. Similar observation is also true for the reorganization energies where restricted B3LYP method produces qualitatively incorrect results, while UB3LYP delivers the results which are in line with those estimated for known organic conjugated systems. The doping changes reorganization energy of N-GNRs; λ_+ being always higher than the corresponding λ_- for graphitic type of doping due to the participation of nitrogen atoms in stabilization of the positive charge.

Acknowledgments

We acknowledge the financial support from Program to Support Research and Technological Innovation Projects (PAPIIT) (grant IN-IN100215) and we also would like to thank the General Direction of Computing and Information Technologies and Communication of the National Autonomous University of Mexico (DGTIC-UNAM) for the support to use the supercomputer facilities. A.E. Torres gratefully acknowledges Consejo Nacional de Ciencia y Tecnología (CONACyT) for a graduate scholarship (245467).

References

1 A. K. Geim and K. S. Novoselov, *Nat. Mater.*, 2007, **6** ,183.
2 A. H. Castro Neto, F. Guinea, N.M.R. Peres, K.S. Novoselov and A.K. Geim, *Rev. Mod. Phys.*, 2009, **81**, 109.
3 T.H. Vo, M. Shekhirev, D. A. Kunkel, M.D. Morton, E. Berglund, L. Kong, P. M. Wilson, P. A. Dowben, A. Ender and A. Sinitskii, *Nat. Commun.*, 2014, **5**, 3189.
4 J. Cai, P. Ruffieux, R. Jaafar, M. Bieri, T. Braun, S. Blankenburg, M. Muoth, A. P. Seitsonen, M. Saleh, X. Feng, K. Müllen and R. Fasel, *Nat.*, 2010, **466**, 470.
5 J. Baringhaus, M. Ruan, F. Edler, A. Tejeda, M. Sicot, A. Taleb-Ibrahimi, A. Li, Z. Zhigang Jiang, E. H. Conrad, C. Berger, C. Tegenkamp, W. A. de Heer, *Nature*, 2014, **506**, 349.
6 L. A. Chernozatonskii, P. B. Sorokin and A. A. Artukh, *Russ. Chem. Rev.*, 2014, **83**, 251.
7 D. Usachov, O. Vilkov, A. Grüneis, D. Haberer, A. Fedorov, V. K. Adamchuk, A. B. Preobrajenski, P. Dudin, A. Barinov, M. Oehzel, C. Laubschat and D.V. Vyalikh, *Nano Lett.* 2011, **11**, 5401.
8 D.Y. Usachov, A. V. Fedorov, O.Y. Vilkov, B.V. Senkovskiy, V.K. Adamchuk, B. V. Andryushechkin and D. V. Vyalikh, *Phys. Solid. State*, 2013, **55**, 1325.
9 R. Peköz and S. Erkoc, *Physica E*, 2009, **42**, 110.
10 J. Zeng, K. Q. Chen, J. He, Z. Q. Fan and X. J. Zhang, *J. Appl. Phys.*, 2011, **109**, 124502.
11 S. S. Chauhan, P. Srivastava and A. K. Shrivastava, *Appl. Nanosci.*, 2014, **4**, 461.
12 T. H. Vo, M. Shekhirev, D.A. Kunkel, F. Orange, M. J.-F. Guinel, A. Enders and A. Sinitskii, *Chem.Commun.* 2014, **50**, 4172.
13 M. Bendikov, H. M. Duong, K. Starkey, K. N. Houk, E. A. Carter and F. Wudl, *J. Am. Chem. Soc.* 2004, **126**, 7416.
14 D. Jiang and S. J. Dai, *Phys. Chem. A*, 2008, **112**, 332.
15 F. Plasser, H. Pašalić, M. H. Gerzabek, F. Libisch, R. Reiter, J. Burgdörfer, T. Müller, R. Shepard and H. Lischka, *Angew. Chem. Int.*, 2013, **52**, 2581.
16 B. Hajgato, D. Szieberth, P. Geerlings, F. De Proft and M.S. Deleuze, *J. Chem. Phys.*, 2009, **131**, 224321.
17 B. Hajgato, M. Huzak and M.S. Deleuze, *J. Phys. Chem. A*, 2011, **115**, 9282.
18 M. Huzak, M.S. Deleuze and B. Hajgato, *J. Chem. Phys.*, 2011, **135**, 104704.
19 B. Hajgató, M.S. Deleuze, *Chem. Phys. Lett.*, 2012, **553** 6.
20 M. S. Deleuze, M. Huzak, B. Hajgató, *J. Mol. Mod.*, 2013, **417**, 17.
21 A. E. Torres, P. Guadarrama and S. Fomine, *J. Mol. Model.*, 2014, **20**, 2208.
22 S. Grimme, J. Antony, S. Ehrlich and H. Krieg, *J Chem. Phys.*, 2010, **132**, 154104.
23 TURBOMOLE V6.5 2013, a development of University of Karlsruhe and Forschungszentrum Karlsruhe GmbH, 1989–2007, TURBOMOLE GmbH, since 2007; available from http://www.turbomole.com
24 T.H. Dunning Jr., *J Chem. Phys.*, 1989, **90**, 1007.
25 S. Grimme *J. Chem. Phys*., 2006, **124**, 034108.
26 R. Ditchfield, W.J. Hehre and J. Pople, *J. Chem. Phys.*, 1971, **54**, 724.
27 M.J. Frisch et al., 2013, Gaussian 09, revision D.01. Gaussian Inc, Wallingford.
28 J. Cai, P. Ruffieux, R. Jaafar, M. Bieri, T. Braun, S. Blankenburg, M. Muoth, A. P. Seitsonen, M. Saleh, X. Feng, K. Müllen and R. Fasel, *Nature,* 2010, **466**, 470.

29 D. Usachov, O. Vilkov, A. Grüneis, D. Haberer, A. Fedorov, V. K. Adamchuk, A. B. Preobrajenski, P. Dudin, A. Barinov, M. Oehzelt, C. Laubschat and D. V. Vyalikh, *Nano Lett.*, 2011, **11**, 5401.
30 H. Wang, T. Maiyalagan and X. Wang, *ACS Catal.*, 2012, **2**, 781.
31 R. Lv, Q. Li, A. R. Botello-Méndez, T. Hayashi, B. Wang,A. Berkdemir, Q. Hao, A. L. Elías, R. Cruz-Silva, H. R. Gutiérrez, Y. A. Kim, H. Muramatsu, J. Zhu, M. Endo, H. Terrones, J.-C. Charlier, M. Pan and M. Terrones, *Sci. Rep.*, 2012, **2**, 586.
32 Y-R. Luo, *Comprehensive Handbook of Chemical Bond Energies*, CRC Press, Boca Raton, FL, 2007.
33 H. Hibino, H. Kageshima, M. Kotsugi, F. Maeda, F.-Z. Guo, and Y. Watanabe, *Phys. Rev. B*, 2009, **79**, 125437.
34 A. Rehaman, M. Shahi, C. J. Cramer and L. Gagliardi, *Phys. Chem. Chem. Phys.*, 2009, **11**, 10964.
35 R. González-Luque, M. Merchfin, P. Borowski, and B. O. Roos, *Theor. Chim. Acta,* 1993, **86**, 467.
36 W. Senevirathna, C.M. Daddario and G. Sauvé, *J. Phys. Chem. Lett.* 2014, **5**, 935.
37 B.C. Lin, C.P. Cheng and Z.P.M. Lao, *J. Phys. Chem. A*, 2003, **107**, 5241.
38 M. Malagoli and J. L. Brédas, Chem. Phys. Lett., 2000, 327, 13.
39 K. Sakanoue, M. Motoda, M. Sugimoto and S. Sakaki, *J. Phys. Chem. A*, 1999, **103**, 5551.
40 M. Y. Han, J. C. Brant and P. Kim. *Phys. Rev. Lett.*, 2010, **104**, 056801.
41 N. E. Gruhn, D. A. da Silva, T. G. Bill, M. Malagoli, V. Coropceanu, A. Kahn and J. L. Brédas, *J. Am. Chem. Soc.*, 2002, **124**, 7918.
42 X. Amashukeli, J. R. Winkler, H. B. Gray, N. E. Gruhn and D. L. Lichtenberger, *J. Phys. Chem. A,* 2002, **106**, 7593.